Contrasting Photoinduced Electron-Transfer Properties of Two Closely Related, Rigidly Linked Porphyrin−Quinone Dyads

John P. Sumida, Paul A. Liddell, Su Lin, Alisdair N. Macpherson, Gilbert R. Seely, Ana L. Moore,* Thomas A. Moore,* and Devens Gust*

Center for the Study of Early Events in Photosynthesis, Department of Chemistry and Biochemistry, Arizona State University, Tempe, Arizona 85287-1604

Received: November 4, 1997; In Final Form: February 10, 1998

Two closely related, rigidly linked porphyrin−naphthoquinone dyads have been prepared and studied using time-resolved fluorescence and absorption methods. Dyad **1**, whose quinone carbonyl groups are relatively close to the porphyrin macrocycle, exhibits photoinduced electron-transfer rate constants that are virtually independent of solvent dielectric constant and temperature within the range 77−295 K. Dyad **2**, which has a similar donor−acceptor linkage but whose quinone carbonyl groups are ∼2 Å farther from the porphyrin, features photoinduced electron-transfer rate constants that decrease with decreasing solvent dielectric constant. Electron transfer in this molecule ceases at low temperatures. Photoinduced electron transfer in dyad **2** exhibits the usual dependence on free energy change and solvent reorganization observed in many similar porphyrin−quinone systems. The behavior of **1** may be attributed at least in part to the smaller separation of the porphyrin radical cation and the quinone radical anion, which leads to nearly barrierless electron transfer and makes transfer less susceptible to effects due to changes in solvent dielectric properties and temperature. Charge recombination rates in the dyads are substantially slower than charge separation rates, unlike those of many porphyrin−quinone systems. This suggests that these molecules might be useful as components of more complex molecular devices.

Introduction

In contrast to photosynthetic reaction centers, which demonstrate photoinduced electron-transfer behavior that is relatively insensitive to temperature and thermodynamic driving force,[1−5] most synthetic reaction center models display electron-transfer rates that are strongly dependent upon free energy change and environmental factors. The most thoroughly studied class of artificial reaction centers features porphyrin moieties covalently linked to quinone acceptors.[1,6−10] In most of these molecules (but not all[7,11−16]), photoinduced electron transfer is rapid in reasonably polar solvents at ambient temperatures but is not observable at low temperatures. In addition, electron transfer usually slows significantly as solvent polarity is decreased.

We recently reported the preparation and spectroscopic study of rigidly linked porphyrin−quinone dyad **1**.[17] Photoinduced electron transfer from the porphyrin first excited singlet state to the quinone occurs with rate constants of $\sim 10^{12}$ s^{-1} in solvents ranging in dielectric constant from ∼2.0 to 25.6 and at temperatures from 77 to 295 K. The transfer rate is also relatively insensitive to changes in thermodynamic driving force of up to 0.4 eV. The behavior of this molecule is phenomenologically more similar to photosynthetic electron transfer than is that of the majority of model systems. To better define the structural features that give rise to this, we have now prepared and studied dyad **2**. Although the structural relationship of **2** to **1** is quite close, the two molecules show very different photoinduced electron-transfer characteristics.

Results

Synthesis. The dyads were prepared by the Diels−Alder reaction of appropriate quinones and porphyrin diene precursors.

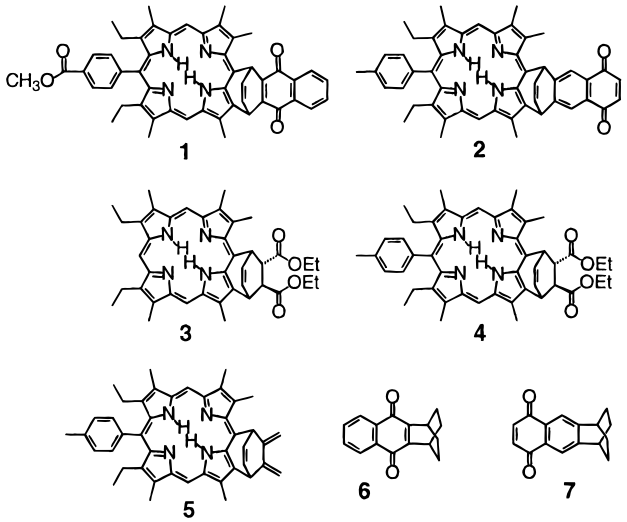

The syntheses of **1** and model porphyrin **3** have been previously reported.[17,18] The preparation of **2** and model porphyrin **4** is described in the Experimental Section.

Molecular Conformation. Dyads **1** and **2** share the same bicyclic bridge linking the porphyrin and quinone moieties, and this bridge precludes any large-scale molecular motions that could modulate interchromophore separations, angles, or electronic coupling interactions. Molecular modeling allows estimation of the distance from the center of the porphyrin ring of **2** to the center of the six-membered ring bearing the quinone moiety as 8.8 Å. The corresponding distance in **1** is 6.7 Å.[17] In both molecules, the dihedral angle between the plane of the porphyrin and that of the quinone is ∼120°.

S1089-5639(98)00068-1 CCC: $15.00
Published on Web 03/28/1998

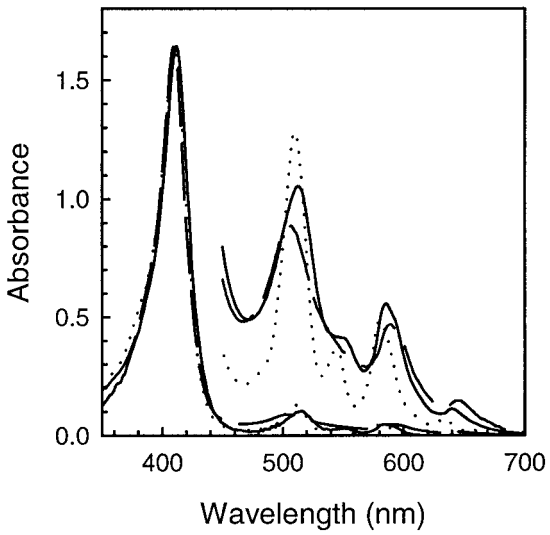

Figure 1. Absorption spectra of model porphyrin **4** (···) and dyads **1** (- - -) and **2** (—) in 2-methyltetrahydrofuran solution. The spectra have been normalized at the Soret band in the 410 nm region, and the inset is a 10-fold expansion.

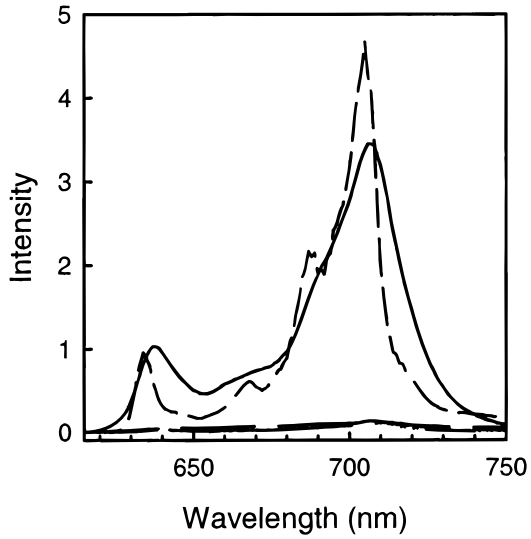

Figure 2. Fluorescence emission spectra of ~1 × 10^{-5} M 2-methyltetrahydrofuran solutions of model porphyrin **4** at 298 K (—) and of dyad **2** at 298 K (-·-), 190 K (-···-), 181 K (···), 159 K (— —), and 91 K (- - -). Excitation was at 590 nm.

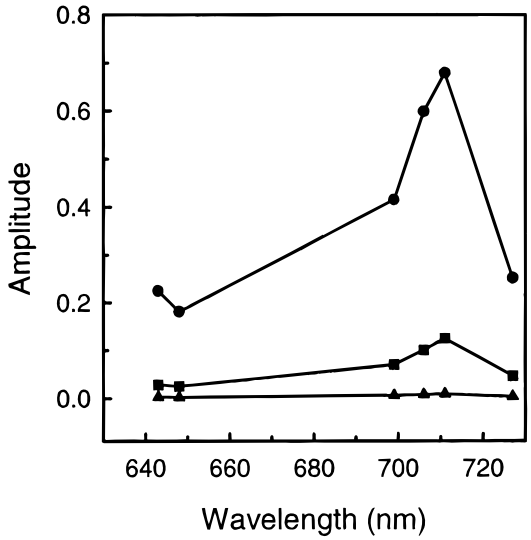

Figure 3. Decay-associated spectra showing components of the decay of the first excited singlet state of dyad **2** following 590 nm excitation of a ~1 × 10^{-5} M solution in 2-methyltetrahydrofuran. Global analysis at the indicated wavelengths ($\chi^2 = 1.12$) gave exponential decays with lifetimes of 0.005 (●), 0.036 (■), and 9.98 ns (▲).

Electrochemistry. Cyclic voltammetric studies of **2** in benzonitrile solution yielded a quasireversible first oxidation potential for the porphyrin of +0.393 V vs a ferrocene internal reference redox system. The first reduction of the quinone moiety was reversible, at −1.116 V. The corresponding first oxidation and reduction potentials for dyad **1** are +0.422 and −1.148 V, respectively.[17]

Steady-State Absorption Spectra. The absorption spectra of **1**, **2**, and **4** in 2-methyltetrahydrofuran are shown in Figure 1. Model porphyrin **4** has a Soret maximum at 409 nm and Q-bands at 510, 546, 580, and 634 nm. The Soret band of **2** at 411 nm is similar to that of **4**, but the Q-bands at 513, 550 (shoulder), 586, and 640 nm are broadened significantly and the maxima are shifted to longer wavelengths. A slightly greater degree of broadening of the Q-bands is observed for dyad **1**, whose absorption maxima are found at 409, 507, 589, and 646 nm. The absorption spectra of **2** in benzonitrile, dichloromethane, 2-methyltetrahydrofuran, toluene, and benzene are essentially identical.

Steady-State Fluorescence Spectra. In 2-methyltetrahydrofuran, porphyrin **4** has fluorescence emission maxima at 638 and 705 nm (Figure 2). The quantum yield is 0.065, as determined by the comparative method using *meso*-tetraphenylporphyrin as the standard.[19] Solutions of **2** in 2-methyltetrahydrofuran at 298, 190, 181, or 159 K show very weak emission (Figure 2), most of which is due to minor impurities. When the sample is cooled to 91 K, strong emission is observed ($\Phi = 0.055$). The emission maxima occur at 634, 668, 687, and 705 nm. The fluorescence quenching of **2** at ambient temperature is indicative of photoinduced electron transfer to form the $P^{\bullet+}-Q^{\bullet-}$ charge-separated state. At 91 K, significant electron transfer no longer occurs, as evidenced by the large increase in fluorescence quantum yield.

Time-Resolved Fluorescence Studies. A 2-methyltetrahydrofuran solution of **4** was excited with 9 ps laser pulses at 590 nm, and its fluorescence decay was measured using the time-correlated single photon counting technique. The fluorescence, detected at 663 nm, decayed as a single exponential with a lifetime of 10.1 ns ($\chi^2 = 1.08$). A similar solution of dyad **2** was excited, and fluorescence was detected at six wavelengths in the 640−730 nm region. The decays were analyzed globally as three exponentially decaying components with lifetimes of 0.005, 0.036, and 9.98 ns (Figure 3). The major component, with a lifetime of 5 ps, is assigned to the decay of **2**, and the two minor components are assigned to impurities. Thus, the first excited singlet state of the porphyrin of **2** is quenched by photoinduced electron transfer to the attached quinone, as also shown by the steady-state experiments.

Similar experiments were carried out in benzonitrile, dichloromethane, toluene, and benzene, where the major component of the fluorescence decay had lifetimes of 0.001, 0.001, 0.015, and 0.008 ns, respectively. The lack of solubility in aliphatic hydrocarbons precluded studies in such media. All of the fluorescence lifetimes measured for **2** are well within the instrument response function of 0.035 ns, decreasing the accuracy of the measurement. The very short lifetimes in benzonitrile and dichloromethane are especially vulnerable. We turned to time-resolved absorption spectroscopy in order to obtain more accurate estimates of the singlet-state lifetimes and to detect the products of electron transfer.

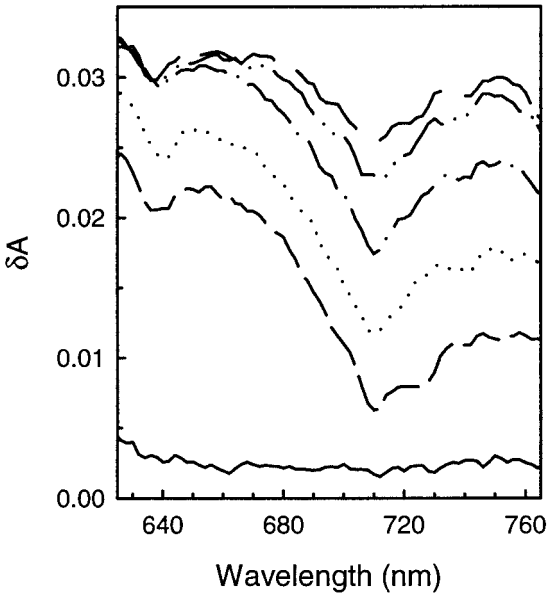

Figure 4. Representative transient absorption spectra at early times after excitation of a $\sim 5 \times 10^{-4}$ M solution of dyad **2** in 2-methyltetrahydrofuran with a ~150 fs laser pulse at 590 nm. Spectra were obtained at −0.6 (—), 0.8 (- - -), 1.6 (···), 3.2 (-·-), 6.4 (-···-), and 12.8 ps (- -) ps after excitation.

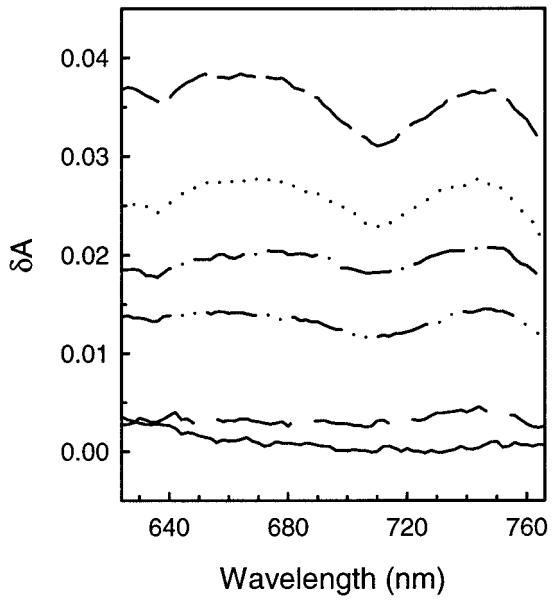

Figure 5. Representative transient absorption spectra at later times after excitation of a $\sim 5 \times 10^{-4}$ M solution of dyad **2** in 2-methyltetrahydrofuran with a ~150 fs laser pulse at 590 nm. Spectra were obtained at −1.0 (—), 13.0 (- - -), 20.0 (···), 30.0 (-·-), 40.0 (-···-), and 50.0 ps (− −) after excitation.

Time-Resolved Absorption Studies. Excitation of $\sim 5 \times 10^{-4}$ M 2-methyltetrahydrofuran solutions of porphyrin **3** with 150−200 fs, 590 nm laser pulses resulted in the immediate appearance of the transient absorption spectrum of the porphyrin first excited singlet state.[17] In the 625−760 nm region, this spectrum is characterized by stimulated emission bands at 630 and 700 nm superimposed upon the broad, featureless absorption of the excited state. The spectrum rises with a time constant of 0.26 ps, which is close to the excitation pulse width, and does not decay appreciably on the time scale of several hundred picoseconds.

At early times, the transient spectrum of dyad **2** in the 625−765 nm region is similar to that for **3**, with stimulated emission at 640 and 710 nm superimposed on a broad absorption (Figure 4). At later times the stimulated emission, the signature of the porphyrin first excited singlet state, disappears, and only a broad, relatively featureless absorption is observed (Figure 5). This absorption is characteristic of the porphyrin radical cation of the $P^{\bullet+}-Q^{\bullet-}$ state. The time dependence of the spectrum at 690 ± 10 nm is shown in Figure 6. The prompt rise of ^1P-Q with the laser pulse is followed by the exponential growth of the $P^{\bullet+}-Q^{\bullet-}$ state with a time constant of 5.9 ps (Figure 6a), which is consistent with the measured fluorescence lifetime for ^1P-Q of 5 ps. The charge-separated state decays exponentially with a lifetime of 29 ps (Figure 6b).

Similar experiments were carried out in benzonitrile, dichloromethane, toluene, and benzene. The results are reported in Table 1. The precision of the rate constants $>1 \times 10^{12}$ s^{-1} is less than that of the smaller rate constants due to convolution with the excitation pulse and rise of the porphyrin first excited singlet state.

Photoinduced Electron Transfer. The results for dyad **2** can be interpreted in terms of Figure 7. The energetics shown are based on the electrochemical measurements in benzonitrile, which allow estimation of the energy of the $P^{\bullet+}-Q^{\bullet-}$ charge-separated state as 1.51 eV above the ground state. In this estimate, no correction is made for any Coulombic effects. The energy of the corresponding state in **1** is 1.57 eV.

The porphyrin first excited singlet state of **2** decays by the usual photophysical pathways of internal conversion, intersystem crossing, and fluorescence. Assuming that linking the quinone to the porphyrin does not greatly perturb these pathways, the sum of the rate constants for these processes (k_1, the rate constant for step 1 in Figure 7) may be estimated as the reciprocal of the singlet lifetime of model porphyrin **4**. In 2-methyltetrahydrofuran, the time-resolved fluorescence studies give a value for k_1 of 9.9×10^7 s^{-1}. The ^1P-Q state also decays by photoinduced electron transfer to yield $P^{\bullet+}-Q^{\bullet-}$. The rate constant for photoinduced electron transfer, k_2, is given by eq 1, where k_{rise} is the reciprocal of the time constant for formation of $P^{\bullet+}-Q^{\bullet-}$ and decay of ^1P-Q (Table 1).

$$k_2 = k_{rise} - k_1 \quad (1)$$

In all of the solvents investigated here, k_{rise} is much larger than k_1, and k_2 equals k_{rise} within experimental error. In 2-methyltetrahydrofuran, for example, k_2 for **2** equals 2×10^{11} s^{-1}. The $P^{\bullet+}-Q^{\bullet-}$ state decays to the ground state by charge recombination step 3; k_3 equals the experimentally observed k_{decay} value in Table 1. The table also lists k_{rise} (=k_2) and k_{decay} (=k_3) values for **1**.[17]

Discussion

Comparison of Results for Dyads 1 and 2. Although dyads **1** and **2** are very similar in structure, their electron-transfer behavior is quite different. Photoinduced electron-transfer rates in **1** are large and essentially independent of solvent. Photoinduced electron transfer is also essentially independent of temperature, with no observable change in rate constant over the range 77−295 K.[17] In dyad **2**, the rate constant for photoinduced electron transfer in benzonitrile is slightly larger than that for **1**. However, the rate constant decreases by about 1 order of magnitude in going from polar to nonpolar solvents. In addition, the photoinduced electron-transfer rate in **2** is strongly temperature dependent. The steady-state fluorescence results show that transfer is very fast down to at least 159 K but that by 91 K electron transfer has slowed dramatically or

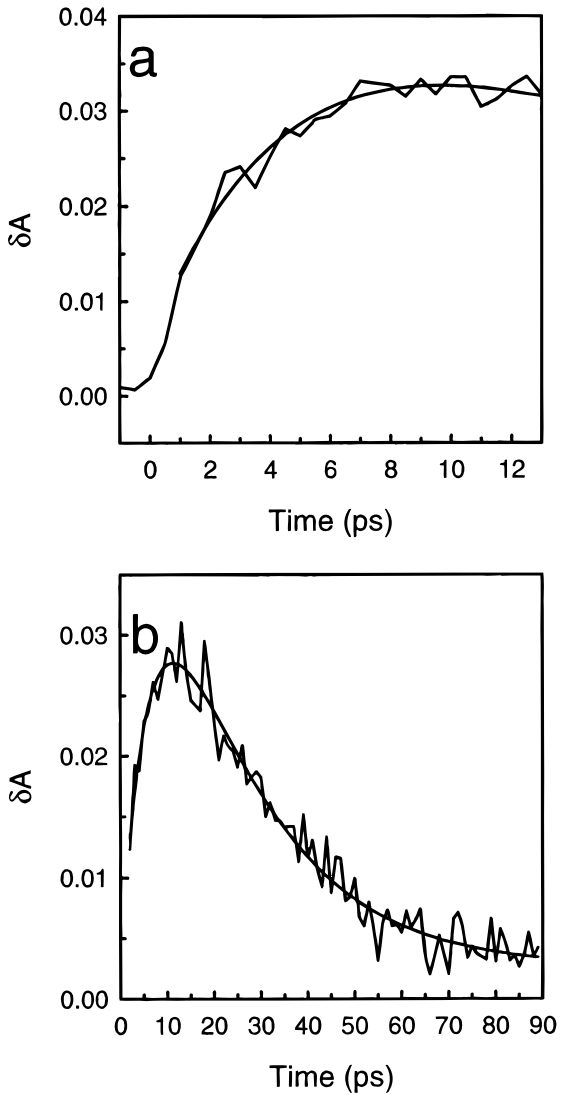

Figure 6. (a) Rise of the transient absorption at 690 ± 10 nm after excitation of a ~5 × 10^{-4} M solution of dyad **2** in 2-methyltetrahydrofuran with a ~150 fs laser pulse at 590 nm. The smooth line is a least-squares fit of the slow part of the rise and the decay to exponential functions. The time constant for the rise is 5.9 ps. (b) Rise and decay of the transient absorption in the same spectral region measured on a longer time scale. The smooth line is a least-squares fit of the rise and decay to exponential functions and yields a decay time constant of 29 ps.

TABLE 1: Rate Constants for the Rise and Decay of the Charge-Separated State in Porphyrin−Quinone Dyads 1 and 2 as a Function of Solvent

		dyad **1**		dyad **2**	
solvent	ϵ	k_{rise} (s^{-1})	k_{decay} (s^{-1})	k_{rise} (s^{-1})	k_{decay} (s^{-1})
benzonitrile	25.60	8×10^{11}	2×10^{11}	1×10^{12}	2×10^{11}
dichloromethane	9.08	3×10^{12}	5×10^{11}	1×10^{12}	5×10^{11}
2-methyltetrahydrofuran	7.60	1×10^{12}	7.7×10^{10}	2×10^{11}	4.9×10^{10}
toluene	2.38	1×10^{12}	4.4×10^{10}	8.0×10^{10}	9.0×10^{9}
benzene	2.28	7×10^{12}	4.2×10^{10}	2×10^{11}	1.2×10^{10}

ceased, and the quantum yield of fluorescence from the dyad approaches that of the model porphyrin. Why do two dyads that are so closely related structurally have such different photoinduced electron-transfer behavior? Several aspects of this question will be addressed below.

Optical Electron Transfer. Electron transfer sometimes occurs by an optical transition from the ground state directly into an absorption band of a charge-transfer state. The very rapid photoinduced electron transfer observed for **1** and the perturbation of the absorption spectrum upon linking the donor and acceptor might be indicative of such behavior. The transient absorption of the $P^{\bullet+}-Q^{\bullet-}$ state in **1** rises only slightly more slowly than the excitation pulse width in all solvents, and no clear-cut spectral signature for the local excited state was observed.

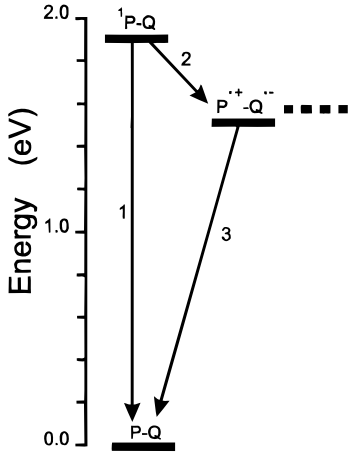

Figure 7. Relevant high-energy states of dyad **2** and their interconversion pathways. The energetics were derived from spectroscopic and cyclic voltammetric measurements. The dashed line represents the $P^{\bullet+}-Q^{\bullet-}$ state for dyad **1**.

The transient absorption results for **2** clarify the situation. The perturbation of the ground-state absorption in the Q-band region is present in **2** to only a slightly lesser extent than in **1** (Figure 1). Thus, if this perturbation is due to charge-transfer absorption, both molecules should demonstrate optical electron transfer. However, the transient absorption spectra for **2** (Figures 4 and 5) clearly show the initial formation of the local excited state ^1P-Q and the slower conversion of this state into $P^{\bullet+}-Q^{\bullet-}$. On this basis, charge-transfer absorption can be ruled out.

Electronic Coupling. Differences in electronic coupling might contribute to the divergent behavior of **1** and **2**. The effect of coupling may be conveniently discussed in terms of eq 2[20−22] and similar equations[23,24] that have been developed for nonadiabatic electron-transfer reactions. The electron-transfer rate constant is k_{et}.

$$k_{et} = \sqrt{(\pi/\hbar^2 \lambda k_B T)}\,|V|^2 \exp[-(\Delta G^\circ + \lambda)^2/4\lambda k_B T] \quad (2)$$

The preexponential factor includes the electronic matrix element V that describes the coupling of the reactant state with that of the product. In addition to Planck's constant, Boltzmann's constant k_B, and the absolute temperature T, this factor also includes the reorganization energy for the reaction, λ. It is convenient to express λ as the sum of an internal energy, λ_i, and the solvent reorganization energy, λ_s. The exponential term also includes the standard free energy change for the reaction, ΔG°. Equation 2 predicts an increase in rate with thermodynamic driving force (the "normal" region) up to a maximum when $-\Delta G^\circ = \lambda$ and a decrease in rate as the standard free energy change becomes more negative in the "inverted" region.

The electronic matrix element V defines an upper limit to the electron-transfer rate when $-\Delta G^\circ$ equals λ. In the dyads V is related to the electronic coupling between the porphyrin and the quinone, which occurs across the bicyclic bridge joining the two moieties. Even though the bridging carbons are

saturated, the interaction through bridges of this type may be relatively strong.[25−27] The coupling in **1** and **2** might be expected to be comparable, as the bridge and porphyrin macrocycles are identical. However, some differences still arise because the interaction involves different naphthoquinone π-orbitals in the two molecules. To investigate the magnitude of this effect, AM1 calculations were performed on quinone models **6** and **7**. To a first approximation, V depends on the square of the LUMO wave function at the quinone carbon atoms bearing the bridge. This value for the corresponding carbon atoms in **6** and **7** is 0.107 and 0.054, respectively. This suggests that V^2, and therefore k_{et}, is about 4 times larger for **1** than for **2**.

The experimental data suggest that the electronic interactions are comparable for the two dyads. The photoinduced electron-transfer rate constants in polar solvents (dichloromethane or benzonitrile) are nearly identical in the two species ($\sim 10^{12}$ s^{-1}). The nominal $\Delta G°$ values, estimated from the absorbance spectra and electrochemical measurements, are similar for the two dyads in polar solvents. If we assume that λ is also similar for the two molecules in polar solvents (but vide infra), then eq 2 suggests that the values of V for **1** and **2** must be roughly the same as well. Although some differences in electronic coupling must exist, the explanation for the strongly divergent behavior of the two molecules seems to lie elsewhere.

Thermodynamic Driving Force, Reorganization Energy, and Solvent Effects. The spectroscopic and electrochemical data indicate that in polar solvents $\Delta G°$ for charge separation is similar in both dyads (−0.35 eV in **1** and −0.42 eV in **2**). Equation 2 predicts that, on the basis of $\Delta G°$ alone, photoinduced electron transfer should be slightly more rapid in **2** than in **1**. This is the case in benzonitrile, but in less polar solvents, transfer in **1** is much more rapid than it is in **2**. Solvent affects both driving force and reorganization energy. The effect on the free energy change is often discussed in terms of eq 3, which treats the charge-separated state as two spherical ions with radii R_P and R_Q separated by a distance R_{PQ} and immersed in a solvent of dielectric constant ϵ_s.[28−30]

$$\Delta G° = e(E_P - E_Q)_r + \frac{e^2}{4\pi\epsilon_0\epsilon_s}\left[\frac{1}{2R_P} + \frac{1}{2R_Q} - \frac{1}{R_{PQ}}\right] - \frac{e^2}{4\pi\epsilon_0\epsilon_s^r}\left[\frac{1}{2R_P} + \frac{1}{2R_Q}\right] - E_{1_p} \quad (3)$$

The quantities E_P and E_Q are the first oxidation and reduction potentials of the porphyrin and quinone, respectively, as measured electrochemically in a reference solvent of dielectric constant ϵ_s^r, ϵ_0 is the permittivity of free space, E_{1_p} is the energy of the porphyrin first excited singlet state, and e is the electronic charge. Equation 3 has been used successfully to correlate solvent effects on electron transfer in some porphyrin−quinone[30] and porphyrin−porphyrin[31] dyads, but its quantitative applicability to some other porphyrin−quinone systems has been questioned.[29] In addition, the ions in the charge-separated states of the dyads are not spherical, and are separated in part by the bridge, rather than solvent. Despite these limitations, eq 3 provides a useful theoretical framework for discussion of electron transfer in **1** and **2**.

The reorganization energy λ is also solvent-dependent. The internal reorganization energy λ_i for porphyrin−quinone systems has been estimated as $\sim$0.3 eV.[11,15,32] Marcus has proposed that λ_s depends on the static (ϵ_s) and high-frequency ($\epsilon_{op} = n^2$) dielectric constants of the solvent as shown in eq 4.[29,33,34]

$$\lambda_s = \frac{e^2}{4\pi\epsilon_0}\left(\frac{1}{2R_P} + \frac{1}{2R_Q} - \frac{1}{R_{PQ}}\right)\left(\frac{1}{\epsilon_{op}} - \frac{1}{\epsilon_s}\right) \quad (4)$$

The dependence of $\Delta G°$ and λ_s on the separation of the ions predicted by eqs 3 and 4 suggests a partial explanation for the dichotomous behavior of **1** and **2**. We have chosen to use an R_P value of 6 Å and an R_Q value of 4 Å. The center-to-center distances between the porphyrin and quinone are 6.7 Å in **1** and 8.8 Å in **2** based on molecular modeling, but the actual separation of the charges will be less than this because the ions are very polarizable, and the centers of charge will tend to migrate toward one another. This effect will be especially important in **1**, as the ionic separation is smaller.

Figure 8 shows plots of $\Delta G°$ vs ϵ_s (eq 3) for a variety of R_{PQ} values using the E_P, E_Q, and E_{1_p} values appropriate for **1**. For large donor−acceptor separations, $\Delta G°$ increases considerably at low dielectric constant due to loss of solvent dielectric stabilization of the individual ions. As the ionic separation decreases, the driving force becomes less sensitive to decreasing dielectric constant because increased stabilization due to mutual Coulombic attraction of the ions counterbalances this loss of solvent stabilization. The solvent reorganization energy shows similar behavior, becoming small for all values of ϵ_s when R_{PQ} is $\sim$5 Å.

As mentioned above, the internal reorganization energy for porphyrin−quinone systems has been estimated as $\sim$0.3 eV, and in nonpolar solvents, eq 4 yields a solvent reorganization energy for **2** of $\sim$0.1−0.2 eV. In more polar solvents, λ_s increases considerably. The $\Delta G°$ value for **2** in polar solvents is $\sim$−0.4 eV. Thus, electron transfer in **2** occurs in the normal region of eq 2, and the predicted decrease in driving force with decreasing solvent dielectric constant should result in a decrease in electron-transfer rate, as is observed.

In the case of dyad **1**, however, the separation of charges must be less than 6.7 Å and possibly considerably less in nonpolar solvents where Coulombic attraction is most important. Figure 8 shows that, at R_{PQ} values of 5−6 Å, $\Delta G°$ for photoinduced electron transfer increases only very slightly with decreasing solvent dielectric constant. The value of λ_s is small at this ionic separation and nearly invariant with solvent dielectric constant. Thus, in the 5−6 Å range of distances, the very weak dependence of $\Delta G°$ and λ on solvent can lead to photoinduced electron-transfer rates that are essentially independent of solvent dielectric constant. Photoinduced electron transfer in dyad **1** is therefore expected to be relatively immune from solvent influences, whereas dyad **2**, with a larger ionic separation, is subject to solvent effects in the same way as the majority of other porphyrin−quinone systems. Solvent effects on $\Delta G°$ can also be evaluated by treating the charge-separated state as a single dipole in a cavity surrounded by solvent.[35−37] This model is also qualitatively in agreement with the conclusions discussed above.

Temperature Effects. In dyad **2**, electron transfer is very rapid down to at least 159 K and ceases at 91 K and below. This behavior is also consistent with the interpretation outlined above. Figure 2 shows that the increase in fluorescence quantum yield is not uniform with temperature, but occurs rather abruptly between 159 and 91 K. The 2-methyltetrahydrofuran is a liquid at 159 K but a rigid glass at 91 K.[38] Upon freezing, the solvent is converted from a relatively polar mobile medium with a dielectric constant of 7.60 to a rigid glass where the dielectric constant is small ($\sim$2.60[39]). A decrease of this magnitude in solvent dielectric constant would decrease $|\Delta G°|$ for **2** considerably and possibly even make the reaction

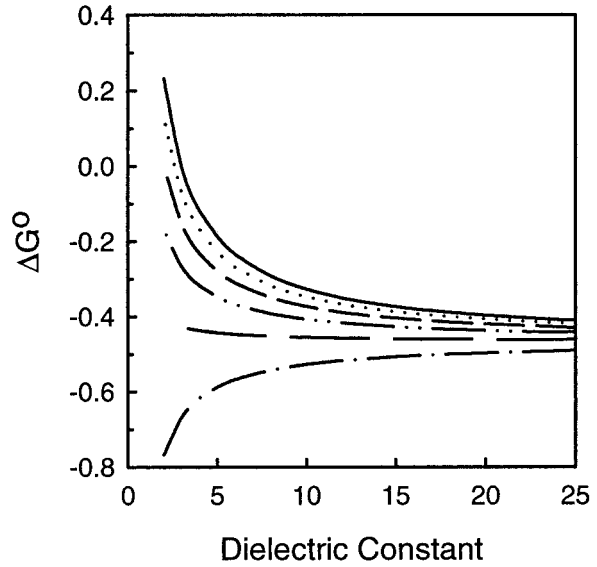

Figure 8. Plot of the dependence of $\Delta G°$ on solvent dielectric constant as per eq 3. The curves represent separations of the porphyrin radical cation and quinone radical anion of 9.0 (—), 8.0 (···), 7.0 (- - -), 6.0 (-···-), 5.0 (— —), and 4.0 Å (-·-). The other parameters are as described in the text.

endergonic. This explains the lack of significant photoinduced electron transfer in **2** at low temperatures.

In **1**, the rate of photoinduced electron transfer is independent of temperature in the range 77−295 K.[17] At 77 K, λ_s is expected to be close to 0 and λ_i remains at ∼0.3 eV. If, as discussed above, $\Delta G°$ for **1** is approximately independent of solvent dielectric constant at the electrochemically determined value of −0.35 eV, then $-\Delta G° \sim \lambda$. If one assumes that this near equivalence of $-\Delta G°$ and λ persists as the effective solvent dielectric constant changes with the transition to the fluid state, as suggested by eqs 3 and 4 when R_{PQ} is small, then the photoinduced electron-transfer rate constant will be nearly temperature invariant, as observed.

These relationships among eqs 2, 3, and 4 have been nicely integrated by Verhoeven, Paddon-Row, and co-workers.[40] Assuming the condition of $-\Delta G° = \lambda$, they have derived eq 5 for P_{opt}, which is, for a given system, the free energy change (as measured spectro- and electrochemically in polar solvents) that will make electron transfer optimally rapid and virtually barrierless in all solvents. The distance r is the

$$P_{opt} \approx -\lambda_i - \frac{e^2}{\epsilon_{op}}\left(\frac{1}{r} - \frac{1}{R_{CC}}\right) \qquad (5)$$

average ionic radius and R_{CC} is the center-to-center distance between the donor and acceptor (R_{PQ} in the present case). We may apply eq 5 to dyad **1** by first assuming that $P_{opt} = -0.35$ eV. That is, we assume that in dyad **1** structural and driving force conditions are already optimal for barrierless electron transfer in all solvents, as suggested by the spectroscopic results. We can then set $\lambda_i = 0.3$ eV, $R_{CC} = 6.7$ Å, and $\epsilon_{op} = 2$ (an average value for typical organic solvents) and evaluate eq 5 for the average ionic radius r. The value obtained, 6.5 Å, may then be used to calculate P_{opt} for dyad **2**, where $R_{CC} = 8.8$ Å. The equation yields a P_{opt} value of −0.59 eV. The actual value for the driving force in polar solvents is −0.42 eV. Thus, with **2**, photoinduced charge separation occurs in the normal region of the Marcus relationship and shows the expected dependence on temperature and solvent.

The close proximity of the ions in **1** relative to **2** helps explain the differences in behavior of the two molecules. However, this may not be the whole story. The photoinduced electron-transfer rate constants for **1** and its zinc analogue are nearly the same, even though the driving force is larger in the zinc compound by ∼0.4 eV. It is difficult to rationalize this observation solely on the basis of eqs 3 and 4. In fact, phenomenologically, photoinduced electron transfer in **1** resembles an internal relaxation process that is independent of solvent, temperature, and driving force.[17]

Charge Recombination. In both dyads, charge recombination is slower than charge separation. The recombination rate increases as the dielectric constant of the solvent increases. This behavior is typical of electron transfer in the inverted region of eq 2. As the dielectric constant of the solvent increases, the $P^{\bullet+}-Q^{\bullet-}$ state is stabilized, the reorganization energy increases as per eq 4, and therefore the rate in the inverted region increases. In dyad **2**, the rate of charge recombination varies by a factor of 55 over the range of solvents studied (Table 1). In dyad **1**, however, the range is only a factor of 12. This is consistent with the idea that electron transfer in **1** is less sensitive to solvent properties than in **2** because of the reduced separation of the ions and their insulation from solvent, as discussed above. The details of the charge recombination processes will differ from those of charge separation because charge recombination involves a different set of molecular orbitals, electronic states and energies, and time scales.[17]

Conclusions

Dyads **1** and **2** are very similar in structure, in ground-state absorption properties, and in electrochemical properties as determined by cyclic voltammetry. However, they show quite different electron-transfer behavior. Photoinduced electron transfer in **2** slows with decreasing solvent dielectric constant and ceases in a glass at low temperatures. Charge recombination also slows with decreasing solvent dielectric constant. All of this behavior is consistent with the predictions of eqs 2−4, and similar behavior has been observed for a large number of porphyrin−quinone and other donor−acceptor systems. Photoinduced electron-transfer rates in dyad **1**, on the other hand, are essentially invariant with solvent dielectric constant and temperature. Charge recombination in **1** slows with decreasing solvent dielectric, but the sensitivity of the rate to ϵ_s is less than that observed for **2**.

The behavior of **1** can be rationalized in part by the smaller separation of the ions in the $P^{\bullet+}-Q^{\bullet-}$ state relative to **2**. When the ions are very close together, mutual Coulombic stabilization becomes very important, and stabilization of the ions by solvent becomes less significant. The solvent reorganization energy also becomes small and nearly invariant with solvent dielectric constant. Thus, at the ionic separation in **1**, electron-transfer rates can become essentially independent of solvent properties. The temperature independence of photoinduced electron transfer in **1** is also consistent with this effect, as electron transfer may occur in a regime where $-\Delta G°$ equals λ at all temperatures investigated. The ionic separation may not be the only factor giving rise to the behavior of **1**, as the photoinduced electron-transfer rate constant does not change appreciably when the driving force is increased by ∼0.4 eV through introduction of zinc into the porphyrin.[17] The discussion above suggests that photoinduced electron transfer in the zinc molecule occurs in the inverted region of eq 2 and should therefore be slower than that for **1**. On the other hand, very rapid photoinduced electron transfer has been observed in other zinc-containing porphyrin−

quinone systems,[15,41] and photoinduced electron transfer in zinc-containing porphyrin dyads has been found to lie on a somewhat different rate-vs-free energy change curve than that in their free base analogues.[42] The lack of sensitivity to environmental factors suggests that photoinduced electron transfer in **1** is controlled mainly by intramolecular vibrations. Vibrational overlap terms may play a role either in the context of radiationless transition theory or as limiting factors in the conversion of reactant to product on a quasi-adiabatic potential surface.[17,43]

In both **1** and **2**, charge separation is extremely rapid even in nonpolar solvents, and charge recombination is substantially slower. This is not the case in many porphyrin−quinone systems, where rates of charge recombination exceed those of charge separation, especially in polar solvents.[44] This may be due in part to the rigidity of the porphyrin−quinone linkage, which prevents the molecules from sampling conformations conducive to rapid recombination, and in part to the smaller value of λ in these molecules, relative to dyads with larger separations. Thus, molecules such as these might serve as useful components of more complex molecular devices for conversion of light energy to chemical potential.

Experimental Section

Synthesis. The preparation of dyad[17] **1** and model porphyrin[18] **3** has been previously described.

Porphyrin 4 was prepared as described for a closely related compound.[18] ^{1}H NMR (300 MHz, $CDCl_3$) δ −2.3 (2H, br m, NH), 0.12 (3H, t, J = 7 Hz, $-OCH_2CH_3$), 1.14 (3H, t, J = 7 Hz, 8-CH_2CH_3 or 12-CH_2CH_3), 1.16 (3H, t, J = 7 Hz, 12-CH_2CH_3 or 8-CH_2CH_3), 1.46 (3H, t, J = 7 Hz, $-OCH_2CH_3$), 2.59 (2H, m, $-OCH_2CH_3$), 2.72 (3H, s, Ar−CH_3), 2.73 (2H, q, J = 7 Hz, 12-CH_2CH_3), 2.84 (2H, q, J = y Hz, 8-CH_2CH_3), 3.11 (2H, m, $-OCH_2CH_3$), 3.48 (3H, s, 13-CH_3), 3.57 (3H, s, 7-CH_3), 3.67 (3H, s, 17-CH_3), 3.67 (3H, s, 3-CH_3), 3.83 (3H, s, 18-CH_3), 4.17 (1H, m, −CHCOOEt), 4.40 (2H, q, J = 7 Hz, $-OCH_2CH_3$), 4.45 (1H, m, −CHCOOEt), 5.37 (1H, m, 2^1-H), 7.05 (2H, m, 2^2-H, 2^4-H), 7.35 (1H, m, 2^3-H), 7.46 (2H, m, 10Ar3,5-H), 7.94 (1H, dd, J = 7, 1 Hz, 10Ar2−H or 10Ar6−H), 8.11 (1H, dd, J = 7, 1 Hz, 10Ar6−H or 10Ar2−H), 10.14 (2H, s, 5-H, 15-H); MS m/z 748 (M^+); UV/vis (CH_2Cl_2) 410, 512, 550, 580, 632 nm.

Porphyrin 5 was synthesized from **4** as previously described for a closely related compound.[45] ^{1}H NMR (300 MHz, $CDCl_3$) δ −2.30 (1H, s, NH), −2.21 (1H, s, NH), 1.13 (3H, t, J = 7 Hz, 12 − CH_2CH_3), 1.16 (3H, t, J = 7 Hz, 8 − CH_2CH_3), 2.70 (3H, s, 10Ar4−CH_3), 2.72 (2H, q, J = 7 Hz, 12 − CH_2CH_3), 2.81 (2H, q, J = 7 Hz, 8 − CH_2CH_3), 3.47 (3H, s, $-CH_3$), 3.53 (3H, s, $-CH_3$), 3.63 (3H, s, $-CH_3$), 3.66 (3H, s, $-CH_3$), 3.82 (3H, s, $-CH_3$), 5.29 (1H, s, $=CH_2$), 5.38 (1H, s, $=CH_2$), 5.40 (1H, m, 2^1-H), 5.53 (1H, s, $=CH_2$), 5.61 (1H, s, $=CH_2$), 7.13 (2H, m, 2^2-H, 2^4-H), 7.31 (1H, m, 2^3-H), 7.45 (2H, m, 10Ar3,5-H), 7.97 (1H, d, J = 7 Hz, 10Ar2−H or 10Ar6−H), 8.06 (1H, d, J = 7 Hz, 10Ar6−H or 10Ar2−H), 10.09 (1H, s, 5-H or 15-H), 10.11 (1H, s, 15-H or 5-H); MS m/z 628 (M^+); UV/vis (CH_2Cl_2) 412, 514, 550, 582, 634 nm.

Dyad 2. To a 50 mL round-bottomed flask equipped with a stir bar and condenser was added 40 mg (0.064 mmol) of porphyrin diene **5**, 10 mL of toluene, and 69 mg (0.64 mmol) of benzoquinone. The flask was flushed with dry nitrogen, and the contents were refluxed for 3 h. The solvent was distilled at reduced pressure, and the excess benzoquinone was removed under high vacuum. The resulting mixture was metalated by dissolving the crude product in 20 mL of dichloromethane and stirring the resulting solution with 3 mL of saturated methanolic zinc acetate. After 30 min, the mixture was diluted with dichloromethane, washed with water, dried over anhydrous sodium sulfate, and filtered. Evaporation of the solvent yielded a mixture of zinc porphyrins, which were dissolved in 6 mL of dimethylformamide. An excess of sodium hydride (10 mg) was added, and the mixture was stirred under a nitrogen atmosphere for 24 h. The resulting pink mixture was diluted with 80 mL of diethyl ether, and the solution washed four times with 50 mL portions of water and then with 50 mL of 2 M hydrochloric acid to remove the zinc. The green reaction mixture was neutralized with aqueous sodium bicarbonate and dried over sodium sulfate, and the solvent was distilled at reduced pressure. The residue was dissolved in 30 mL of dichloromethane and stirred with a 15 mg portion of 2,3-dichloro-5,6-dicyanobenzoquinone. After stirring for 10 min, the reaction mixture was diluted with 50 mL of dichloromethane, washed with aqueous sodium bicarbonate, dried over anhydrous sodium sulfate, and filtered. The solvent was evaporated, and the residue was chromatographed (silica gel, 2% ethyl acetate in toluene) to give 14 mg of **2** (30% yield). ^{1}H NMR (300 MHz, $CDCl_3$) δ −2.29 (1H, s, NH), −2.12 (1H, s, NH), 1.11 (3H, t, J = 7 Hz, 12 − CH_2CH_3), 1.13 (3H, t, J = 7 Hz, 8 − CH_2CH_3), 2.67 (2H, q, J = 7 Hz, 12 − CH_2CH_3), 2.69 (3H, s, 10Ar4−CH_3), 2.78 (2H, q, J = 7 Hz, 8 − CH_2CH_3), 3.44 (3H, s, $-CH_3$), 3.50 (3H, s, $-CH_3$), 3.66 (3H, s, $-CH_3$), 3.69 (3H, s, $-CH_3$), 3.98 (3H, s, $-CH_3$), 5.92 (1H, d, J = 6 Hz, 2^1-H), 6.73 (1H, d, J = 10 Hz, Q−H), 6.78 (1H, d, J = 10 Hz, Q−H), 7.40−7.70 (5H, m, 2^2-H, 2^3-H, 2^4-H, 10Ar3,5-H), 7.90−8.05 (2H, m, 10Ar2,6-H), 8.24 (1H, s, Q−H), 8.28 (1H, s, Q−H), 10.00 (1H, s, 5-H or 15-H), 10.08 (1H, s, 15-H or 5-H); MS (FAB) m/z 733.3514 (calcd for $(M+H)^+$, 733.3543).

Instrumental Techniques. The ^{1}H NMR spectra were recorded on Varian Unity spectrometers at 300 or 500 MHz. Unless otherwise specified, samples were dissolved in deuteriochloroform with tetramethylsilane as an internal reference. High-resolution mass spectra were obtained on a Kratos MS 50 mass spectrometer operating at 8 eV in FAB mode. Ultraviolet−visible spectra were measured on a Shimadzu UV2100U UV−vis spectrometer, and fluorescence spectra were measured on a SPEX Fluorolog using optically dilute samples and corrected. Cyclic voltammetric measurements were carried out with a Pine Instrument company model AFRDE4 potentiostat. The electrochemical measurements were performed in benzonitrile at ambient temperatures with a glassy carbon working electrode, a Ag/Ag^+ reference electrode, and a platinum wire counter electrode. The electrolyte was 0.1 M tetra-*n*-butylammonium hexafluorophosphate, and ferrocene was employed as an internal reference redox system.

Fluorescence decay measurements were performed on $\sim 1 \times 10^{-5}$ M solutions by the time-correlated single photon counting method. The excitation source was a frequency-doubled Coherent Antares 76s Nd:YAG laser routed through a variable beam splitter to pump a cavity dumped dye laser.[46] The instrument response function was 35 ps, as measured at the excitation wavelength for each decay experiment with Ludox AS-40.

Transient absorption measurements on the subpicosecond time scale were made using the pump−probe technique. The sample was dissolved in purified solvent, and the resulting solution was circulated by magnetic stirring in a cuvette having a 2 mm path length in the beam area. Excitation was at 590 nm with 150−200 fs, 8 μJ pulses at a repetition rate of 540 Hz. The signals from the pump and continuum-generated white-light probe beam

were collected by an optical spectrometric multichannel analyzer with a dual diode array detector head.[47]

Acknowledgment. This work was supported by a grant from the Division of Chemical Sciences, Office of Basic Energy Sciences, Office of Energy Research, U.S. Department of Energy (DE-FG03-93ER14404). This is publication 352 from the ASU Center for the Study of Early Events in Photosynthesis.

References and Notes

(1) Bixon, M.; Fajer, J.; Feher, G.; Freed, J. H.; Gamliel, D.; Hoff, A. J.; Levanon, H.; Mobius, K.; Nechushtai, R.; Norris, J. R.; Scherz, A.; Sessler, J. L.; Stehlik, D. *Isr. J. Chem.* **1992**, *32*, 449−455.

(2) Feher, G.; Allen, J. P.; Okamura, M. Y.; Rees, D. C. *Nature (London)* **1989**, *339*, 111−116.

(3) Norris, J. R.; Schiffer, M. *Chem. Eng. News* **1990**, *68*, 22−37.

(4) Woodbury, N. W.; Peloquin, J. M.; Alden, R. G.; Lin, X.; Lin, S.; Taguchi, A. K. W.; Williams, J. C.; Allen, J. P. *Biochemistry* **1994**, *33*, 8101−8112.

(5) Peloquin, J. M.; Williams, J. C.; Lin, X.; Alden, R. G.; Taguchi, A. K. W.; Allen, J. P.; Woodbury, N. W. *Biochemistry* **1994**, *33*, 8089−8100.

(6) Connolly, J. S.; Bolton, J. R. In *Photoinduced Electron Transfer, Part D*; Fox, M. A., Channon, M., Eds.; Elsevier: Amsterdam, 1988; pp 303−393.

(7) Wasielewski, M. R. *Chem. Rev.* **1992**, *92*, 435−461.

(8) Gust, D.; Moore, T. A. *Adv. Photochem.* **1991**, *16*, 1−65.

(9) Gust, D.; Moore, T. A.; Moore, A. L. *Acc. Chem. Res.* **1993**, *26*, 198−205.

(10) Maruyama, K.; Osuka, A.; Mataga, N. *Pure Appl. Chem.* **1994**, *66*, 867−872.

(11) Wasielewski, M. R.; Gaines, G. L., III.; O'Neil, M. P.; Svec, W. A.; Niemczyk, M. P.; Prodi, L.; Gosztola, D. In *Dynamics and Mechanisms of Photoinduced Transfer and Related Phenomena*; Mataga, N., Okada, T., Masuhara, H., Eds.; Elsevier Science Publishers: Amsterdam, 1992; pp 87−103.

(12) Rodriguez, J.; Kirmaier, C.; Johnson, M. R.; Friesner, R. A.; Holten, D.; Sessler, J. L. *J. Am. Chem. Soc.* **1991**, *113*, 1652−1659.

(13) Delaney, J. K.; Mauzerall, D. C.; Lindsey, J. S. *J. Am. Chem. Soc.* **1990**, *112*, 957−963.

(14) Khundkar, L. R.; Perry, J. W.; Hanson, J. E.; Dervan, P. B. *J. Am. Chem. Soc.* **1994**, *116*, 9700−9709.

(15) Heitele, H.; Pollinger, F.; Haberle, T.; Michel-Beyerle, M. E.; Staab, H. A. *J. Phys. Chem.* **1994**, *98*, 7402−7410.

(16) Kamioka, K.; Cormier, R. A.; Lutton, T. W.; Connolly, J. S. *J. Am. Chem. Soc.* **1992**, *114*, 4414−4415.

(17) Macpherson, A. N.; Liddell, P. A.; Lin, S.; Noss, L.; Seely, G. R.; DeGraziano, J. M.; Moore, A. L.; Moore, T. A.; Gust, D. *J. Am. Chem. Soc.* **1995**, *117*, 7202−7212.

(18) Liddell, P. A.; Demanche, L. J.; Li, S.; Macpherson, A. N.; Nieman, R. A.; Moore, A. L.; Moore, T. A.; Gust, D. *Tetrahedron Lett.* **1994**, *35*, 995−998.

(19) Gust, D.; Moore, T. A.; Moore, A. L.; Macpherson, A. N.; Lopez, A.; DeGraziano, J. M.; Gouni, I.; Bittersmann, E.; Seely, G. R.; Gao, F.; Nieman, R. A.; Ma, X. C.; Demanche, L.; Luttrull, D. K.; Lee, S.-J.; Kerrigan, P. K. *J. Am. Chem. Soc.* **1993**, *115*, 11141−11152.

(20) Marcus, R. A. *J. Chem. Phys.* **1956**, *24*, 966−978.

(21) Marcus, R.; Sutin, N. *Biochim. Biophys. Acta* **1985**, *811*, 265−322.

(22) Levich, V. *Adv. Electrochem. Electrochem. Eng.* **1966**, *4*, 249−371.

(23) Jortner, J. *J. Chem. Phys.* **1976**, *64*, 4860−4867.

(24) Jortner, J. *J. Am. Chem. Soc.* **1980**, *102*, 6676−6686.

(25) March, J. *Advanced Organic Chemistry*; Wiley-Interscience: New York, 1992; pp 314−316.

(26) Antolovich, M.; Keyte, P. J.; Oliver, A. M.; Paddon-Row, M. N.; Kroon, J.; Verhoeven, J. W.; Jonker, S. A.; Warman, J. M. *J. Phys. Chem.* **1991**, *95*, 1933−1941.

(27) Wasielewski, M.; Niemczyk, M. P.; Svec, W. A. P. *J. Am. Chem. Soc.* **1985**, *107*, 1080−1082.

(28) Weller, A. *Z. Phys. Chem. (Munich)* **1982**, *133*, 93−98.

(29) Schmidt, J. A.; Liu, J.-Y.; Bolton, J. R.; Archer, M. D.; Gadzekpo, V. P. Y. *J. Chem. Soc., Faraday Trans. 1* **1989**, *85*, 1027−1041.

(30) Gaines, G. L. I.; O'Neil, M. P.; Svec, W. A.; Niemczyk, M. P.; Wasielewski, M. R. *J. Am. Chem. Soc.* **1991**, *113*, 719−721.

(31) DeGraziano, J. M.; Macpherson, A. N.; Liddell, P. A.; Noss, L.; Sumida, J. P.; Seely, G. R.; Lewis, J. E.; Moore, A. L.; Moore, T. A.; Gust, D. *New J. Chem.* **1996**, *20*, 839−851.

(32) Joran, A. D.; Leland, B. A.; Felker, P. M.; Zewail, A. H.; Hopfield, J. J.; Dervan, P. B. *Nature (London)* **1987**, *327*, 508−511.

(33) Marcus, R. A. *Can. J. Chem.* **1959**, *37*, 155−163.

(34) Marcus, R. A. *J. Chem. Phys.* **1965**, *43*, 2654−2657.

(35) Onsager, L. *J. Am. Chem. Soc.* **1936**, *58*, 1486-1493.

(36) Seely, G. R. In *Current Topics in Bioenergetics*; Sanadi, D. R., Vernon, L. P., Eds.; Academic Press: New York, 1978; pp 3−37.

(37) Heitele, H.; Pollinger, F.; Kremer, K.; Michelbeyerle, M. E.; Futscher, M.; Voit, G.; Weiser, J.; Staab, H. A. *Chem. Phys. Lett.* **1992**, *188*, 270−278.

(38) Ling, A. C.; Willard, J. E. *J. Phys. Chem.* **1968**, *72*, 1918−2454.

(39) Furutsuka, T.; Imura, T.; Kojima, T.; Kawabe, K. *Technol. Rep. Osaka University* **1974**, *24*, 367.

(40) Kroon, J.; Verhoeven, J. W.; Paddon-Row, M. N.; Oliver, A. M. *Angew. Chem., Int. Ed. Engl.* **1991**, *30*, 1358−1361.

(41) Asahi, T.; Ohkohchi, M.; Matsusaka, R.; Mataga, N.; Zhang, R. P.; Osuka, A.; Maruyama, K. *J. Am. Chem. Soc.* **1993**, *115*, 5665−5674.

(42) DeGraziano, J. M.; Liddell, P. A.; Leggett, L.; Moore, A. L.; Moore, T. A.; Gust, D. *J. Phys. Chem.* **1994**, *98*, 1758−1761.

(43) Jortner, J.; Bixon, M.; Heitele, H.; Michel-Beyerle, M. E. *Chem. Phys. Lett.* **1992**, *197*, 131−135.

(44) Hung, S.-C.; Lin, S.; Macpherson, A. N.; DeGraziano, J. M.; Kerrigan, P. K.; Liddell, P. A.; Moore, A. L.; Moore, T. A.; Gust, D. *J. Photochem. Photobiol. A: Chem.* **1994**, *77*, 207−216.

(45) Liddell, P. A.; Sumida, J. P.; Macpherson, A. N.; Noss, L.; Seely, G. R.; Clark, K. N.; Moore, A. L.; Moore, T. A.; Gust, D. *Photochem. Photobiol.* **1994**, *60*, 537−541.

(46) Gust, D.; Moore, T. A.; Luttrull, D. K.; Seely, G. R.; Bittersmann, E.; Bensasson, R. V.; Rougée, M.; Land, E. J.; de Schryver, F. C.; Van der Auweraer, M. *Photochem. Photobiol.* **1990**, *51*, 419−426.

(47) Lin, S.; Chiou, H.-C.; Kleinherenbrink, F. A. M.; Blankenship, R. E. *Biophys. J.* **1994**, *66*, 437−445.